

Large Bandwidth Fiber Bragg Gratings for CWDM Systems

Fabiano Kuller, Jean Carlos C. Silva, Paulo de Tarso Neves Jr, Paulo V. Cosmo, Hypolito J. Kalinowski, José L. Fabris, Alexandre A. P. Pohl,
Universidade Tecnológica Federal do Paraná, Av. Sete de Setembro, 3165, 80.230-901 Curitiba, Brazil
corresponding author: pohl@utfpr.edu.br

and Rogério Nogueira
Instituto de Telecomunicações, Campus Universitário de Santiago, P-3810-193, Aveiro, Portugal

Abstract—We report on the fabrication of fiber Bragg gratings with bandwidth in excess of 15 nm for application as filters in CWDM systems and their use in a reconfigurable optical add-drop multiplexer. The gratings were tested in a 2.5 Gbps link and reveal a BER performance comparable to commercial thin film filters, which is the standard technology used in such application.

Index Terms— Optical Fiber Devices, Gratings, CWDM.

I. INTRODUCTION

COARSE WAVELENGTH DIVISION MULTIPLEXING (CWDM) has been widely used in metro and access networks. The International Telecommunications Union (ITU) has standardized the wavelength grid between 1270 and 1610nm and established the wavelength spacing to be 20nm in order to allow the simultaneous transmission of several carriers without the need for cooled laser sources [1]. One of the critical components of a CWDM system is the filter used for demultiplexing the optical carriers. Filters for this application are required to have large and flat bandwidth, low excess loss, high isolation and be of easy fabrication. In particular, the large bandwidth is required to counteract the wavelength drift of the uncooled source and promote crosstalk reduction. Usually CWDM demux's have been fabricated using thin-film technology, which employ bulk optical components, such as GRIN lenses or small beam collimators, and require precision alignment procedures and high-cost assemblies [2]. Recently, alternatives techniques have employed lithographically produced planar diffractive gratings [3] or silica-based planar lightwave circuits [4].

In this work we report on the fabrication of CWDM filters based on fiber Bragg gratings with a bandwidth in excess of 15nm, which can be used either as single devices or arranged in a system to form a CWDM Optical Add Drop Multiplexer [5]. Routinely, FBGs are fabricated through the spatial modulation of the fiber core refractive index using a phase-mask interferometer under UV-laser illumination. For simple grating profiles the inscription is performed in one single step, which requires that the phase-mask and the laser beam remain fixed during the writing procedure. Due to the given constraints, only limited bandwidth gratings are obtained (< 1 nm). Thus, the fabrication of

complex profile gratings is not straightforward and use multistep writing techniques [6, 7, 8]. These techniques are usually employed to produce apodization or chirped gratings, but can also lead to large bandwidth gratings, when fabrication parameters are properly adjusted. In this way, such methods can also be used to fabricate filters with the CWDM requirements. Kashyap *et al* developed a method of concatenating individual chirped gratings by irradiating fiber sections between adjacent gratings with UV radiation to tune the optical phase between sections [6]. Cole *et al* introduced a method to fabricate chirped gratings, where a laser beam is scanned across a uniform phase-mask. As the beam is scanned, the fiber or phase-mask is moved at a much lower velocity than the beam scan [7]. Asseh *et al* presented a technique that stitches small gratings together. A small grating is written, the fiber is translated by a grating period along the interferogram with a high-precision air-bearing linear stage, and then the fiber is irradiated again to produce another grating [8]. For instance, Brenann III *et al* presented a grating for dispersion compensation with one of the highest bandwidths (30 nm) reported, which uses a velocity-controlled approach for moving the fiber and does not require position information for feedback [9]. However, most of these techniques require an accurate control of moving parts, which can be achieved by the employment of high-precision linear stages and feedback signals that are used to precisely align the small gratings together. For instance, one can use the fiber fluorescence generated during the UV-illumination as a feedback to align the phase-mask with the previously written fiber grating [10, 11].

For obtaining the large bandwidth gratings reported in this work we also employed a multistep writing technique. Yet, for obtaining gratings with bandwidth in excess of 15nm our experience showed that it is also necessary to employ a chirped phase-mask, fibers using saturated hydrogen loading and over-exposure to the UV beam. This paper is divided in the following sections: section II describes the fabrication process and section III presents experimental data on the characteristics of the large bandwidth gratings. Section IV reports on the employment of the gratings in a four-channel reconfigurable optical add-drop multiplexer followed by section V with the conclusion.

II. GRATING FABRICATION

The writing system used for the fabrication of fiber gratings is composed of a mode-locked, Q-switched Nd:YAG laser from New Wave Research, with two frequency doubling crystals in order to obtain UV radiation at 266nm. The laser generates pulses with an average energy of 30 mJ at a repetition rate of 20 Hz. The laser beam, after being spatially conditioned by two diaphragms, enters the phase mask interferometer, assembled in the Talbot configuration [12]. The beam diameter is also controlled by an iris, which is positioned just after the laser output. The beam diameter control allows adjustment of the recorded FBG length and it also serves as a way to improve the beam spatial uniformity. The diffraction separated beams are focused on the fiber by means of a fused silica cylindrical lens with a 50.2mm focal length, which is used to increase the laser intensity at the focal

line. The useable width of the interference pattern along the fibre core is about 1.5mm. Both conventional communication grade single-mode fiber (ABC Xtal Ltd.) and commercial photosensitive fiber (Thorlabs, Fibercore) were used for the fabrication. Fibers are hydrogen loaded (typically 100-150atm at room temperature) for no less than 2 weeks prior to grating recording.

Gratings were initially recorded with a uniform phase mask using a step by step process, in which several subgratings are sequentially inscribed in the same fiber. The main difference from conventional grating recording, in our case, is the over-exposure to the UV pattern during the fabrication of each subgrating. For obtaining large bandwidth, gratings are recorded using exposure times from several tens of minutes to several hours. The observed grating growth in each step is similar to type I gratings described in the literature [13, 14], until the reflectivity saturates. From that point on, the grating presents saturated reflectance but we observed that its FWHM increases to a certain extent with the illumination time. The recording is accomplished by illuminating the fiber through the phase-mask until the FWHM bandwidth, which is monitored with the optical spectrum analyzer, stops increasing. The fiber is then manually moved from its position and the angles of the interferometer mirror changed in order to modify the recording wavelength. This is necessary for allowing the grating bandwidth to be further extended to the shorter wavelength range. The process is repeated until the desired bandwidth is achieved, which normally takes between five to seven steps. The grating central wavelength can be controlled using the information on the bandwidth increase previously obtained from the several steps used in the fabrication. A typical spectrum of such a grating fabricated with the uniform phase mask is seen in Fig. 1.

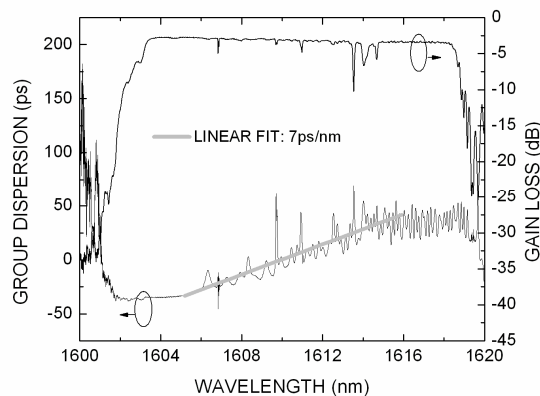


Fig. 1. Typical spectrum of large bandwidth grating fabricated with the uniform phase mask.

Gratings recorded using this process revealed several narrow transmission bands and large group delay ripples on the saturated portion of the spectrum, which is an indication of the phase mismatch occurring between consecutive steps. This poor concatenation is attributed to the difficulty in maintaining a very good alignment of both fiber and the writing beam whilst the fiber is moved

manually from one step to the other.

In an attempt to improve the flatness and to reduce the narrow transmission bands the experimental setup was changed in order to provide for the incident laser beam to be scanned with constant velocity over the phase mask. This modification aimed the improvement of the control and the reduction of misalignments once the fiber remains now fixed at its position during the recording process. Additionally, a chirped phase mask (Ibsen Photonics) of period 1050.5 nm and 10 nm/cm chirp rate was introduced with the purpose of replacing the need for changing the recording wavelength in each step. Indeed, gratings with better flatness were obtained. However, the resulting FWHM bandwidths were not higher than 10nm, due to the usable short length (10mm) of the phase mask, which limited the beam scanning range.

For obtaining bandwidths in excess of 15nm the change of the recording wavelength was reintroduced along with the use of the chirped phase mask, but without scanning the laser beam over the mask. The fabrication takes place again in steps. After the first subgrating is recorded, the position of the beam over the phase mask is changed automatically by the interferometer control to a distance equivalent to the iris diameter (~1mm) and the recording wavelength is modified to fit the desirable range. The process is repeated three to five times until the required bandwidth is achieved, which is controlled by analyzing the grating reflected spectrum in an optical spectrum analyzer. Fig. 02 shows a typical spectrum of a grating recorded using the described technique, where the phase mismatch is reduced as compared to gratings fabricated with the first process.

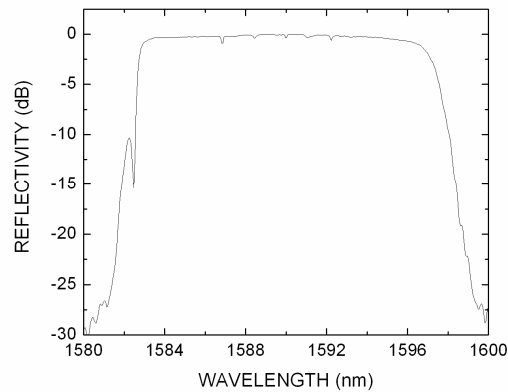


Fig. 2. Typical spectrum of a grating fabricated with the chirped phase mask and the stepwise process.

III. GRATING CHARACTERISTIC

The measurement of excess loss was performed with a simple arrangement using a broadband (ASE) light source, a 3-port optical circulator and a calibrated optical power meter. A reference measurement without the grating is first accomplished so that the excess loss of other components, such as the optical circulator, splices and connectors are previously assessed. The value of the output

optical power at the circulator second port is taken as the reference. The grating is then positioned at this port and the power is measured at its output (in transmission) and at the circulator third port (grating reflected power). The excess loss is estimated by simply subtracting the incident from the grating transmitted plus reflected power at the described ports. Several gratings were measured and insertion losses varied from a minimum 0.5 up to 4 dB. The loss is primarily attributed to scattering and coupling to cladding and radiation modes. The wide observed loss variation, however, seems to be related with fiber misalignments during the fabrication steps, as losses as low as 0.5dB could be obtained in some samples.

The grating dispersion was also estimated through measurements of the group delay using an optical network analyzer with an externally modulated tunable laser source. Fig. 1 also presents the group dispersion behavior of a grating fabricated using the uniform phase-mask. The dispersion coefficient is estimated by a linear best-fit to the measured group delay and gives 7 ps/nm for this particular sample. However, chirped gratings present different dispersion values depending on the port the dispersion is measured [15]. Particularly for large bandwidth gratings the dispersion shows large variations. In our case, some chirped gratings showed dispersion values varying from 20 ps/nm to over 1000 ps/nm.

Bit error rate and isolation tests on the gratings were performed using the set-up shown in Fig. 3. In this case the grating is evaluated considering its application as a drop filter in an optical add-drop multiplexer configuration. The arrangement consists of uncooled DFB lasers that cover the CWDM spectrum from 1470 to 1610nm. The lasers are driven by a pattern generator configured at the 2.5Gbps bit rate. The signal is monitored along the way using optical power monitoring units and an optical spectrum analyzer. By using an optical circulator the signal that is reflected from the grating is dropped and measured with a BER analyzer. Gratings with the central Bragg wavelength at 1490, 1510, 1530 and 1550nm were tested and results presented in Fig. 4. With the exception of the wavelength centered at 1510nm, all other gratings behave similarly requiring about -18.5dBm of power to operate at the 10^{-9} bit error level. The 1510nm central wavelength grating requires about 1.5dB more of power to reach the same performance. For comparison sake, commercial CWDM filters based on the thin-film technology and centered at 1490 and 1510nm were also tested and results shown in the same figure. One sees that the 1490nm TFF presents the same performance as the gratings at the 1490, 1530 and 1550nm. The 1510nm TFF is slightly worse, requiring 0.5dB more of optical power to perform at the same 10^{-9} level.

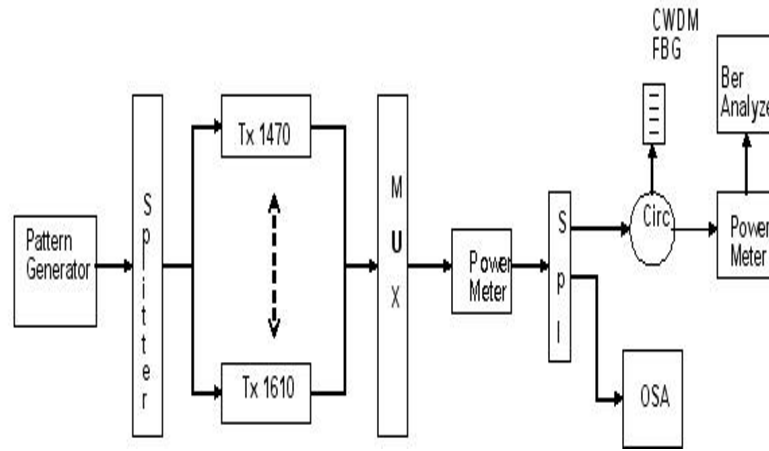


Fig. 3. Experimental arrangement for measuring the BER performance.

Isolation tests were carried out using the optical spectrum analyzer now positioned at the circulator port in place of the power meter. Isolation is measured as the power difference between the peaks of the filtered carrier and the highest level neighbor channel. Best isolation values measured were around -35dB.

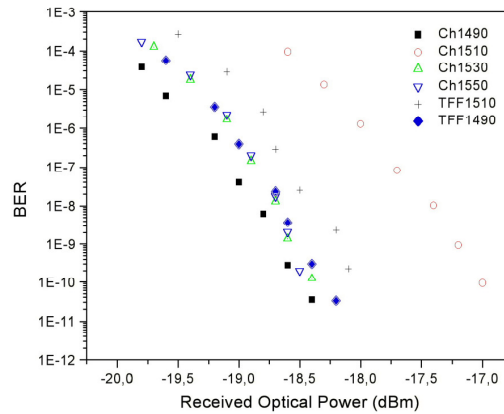


Fig. 4. BER performance of gratings in a CWDM system at 2.5 Gbps.

IV. RECONFIGURABLE OADM WITH LARGE BANDWIDTH GRATINGS

The large-bandwidth gratings were employed in a four-channel reconfigurable optical add drop multiplexer (OADM) designed for operation in a CWDM system. The multiplexer was devised with a serial configuration [16] shown in Fig. 5. It has the advantage of allowing the selection of one or more channels simultaneously. The channel selection is obtained through the use of 1x2 and 2x2 discrete optical switches that are driven by a TTL level signal (represented by A, B,..., E) over a simple turn on-off device. The configuration employs two 1x2 optical switches positioned at the beginning (OSW

1) and end (OSW 5) of the device from left to right in Fig. 5, three 2x2 optical switch (designated OSW 2, OSW 3 and OSW 4, respectively, and positioned after OSW 1), four large bandwidth gratings and two 3-port optical circulators (designated OC 1 and OC 2, respectively). For each additional channel one 2x2 optical switch and one grating are needed. Fig. 5 also shows the logic state of the switches, where “1” means the up-state and “0” the down-state, respectively, for the 1x2 switches and “1” means the bar-state and “0” the cross-bar state, respectively, for the 2x2 switches. In the present demonstration λ_1 , λ_2 , λ_3 and λ_4 correspond to gratings whose Bragg wavelength are centered at 1531, 1550, 1571 and 1592 nm, respectively. The OADM was designed with discrete and connectorized devices for the easy of assembling and demonstration. However, fiber splices should be used in place of the connectors in order to reduce the overall insertion loss.

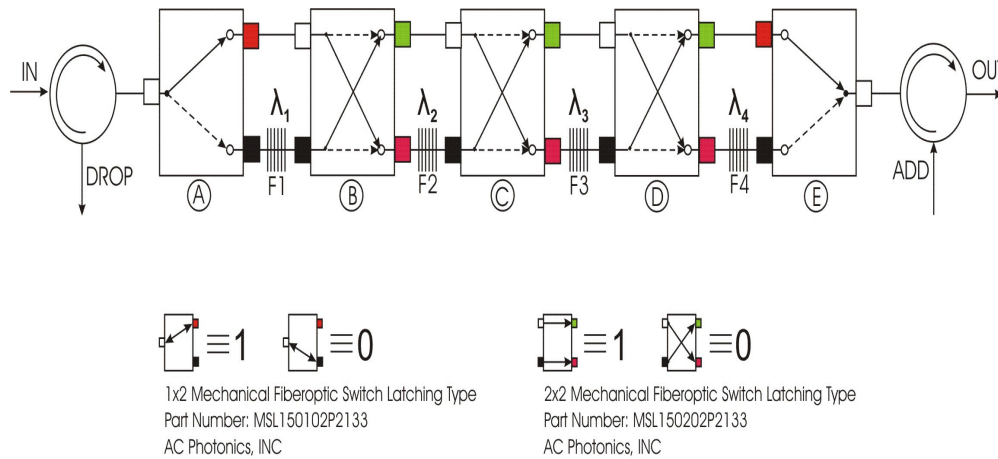


Fig. 5. Configuration of the assembled reconfigurable 4-channel Optical Add drop Multiplexer

The operation of the OADM is as follows. If one wishes to drop only channel λ_2 , per example, the OSW 1 must be set to “1” in order to bypass grating λ_1 ; furthermore, the OSW 2 and OSW 3 must be set to “0” (cross-state) in order to drive the optical signal to grating λ_2 and bypass grating λ_3 , while OSW 4 must be set to “1” (bar-state) in order to bypass grating λ_4 and OSW 5 to “1” to let the optical signal go through to the output circulator OC 2. This way all the channels will pass through the OADM, except λ_2 that will be reflected by the grating FBG 2; the reflected channel λ_2 will return all the way through the same path to the optical circulator OC1 and will be dropped at the OC 1 port. On the other hand, the remaining channels will go forward through the described switch paths and will be available at the output OC 2 port. The add operation occurs at the optical switch OC2 and can be controlled by another switch, which has not been implemented in the present configuration. The assembled OADM allows to add and to drop simultaneously channels of the same wavelength only.

The relationship between the control signals (A, B, C, D and E) and the optical switch states can be previously established by the circuit designer according to the switch pin configuration. An example is given by the setting shown in Table I, which shows the switches logic control table for the OADM.

It establishes all possible paths within the OADM necessary for the selection of a single or several channels simultaneously.

TABLE I. LOGICAL STATES FOR THE SWITCHES

OSW 1	OSW 2	OSW 3	OSW 4	OSW 5	OUT (selected gratings)
1	1	1	1	1	0
0	0	1	1	1	F1
1	0	0	1	1	F2
1	1	0	0	1	F3
1	1	1	0	0	F4
0	1	0	1	1	F1,F2
0	0	0	0	1	F1,F3
0	0	1	0	0	F1,F4
1	0	1	0	1	F2,F3
1	0	0	0	0	F2,F4
1	1	0	1	0	F3,F4
0	1	1	0	1	F1,F2,F3
0	1	0	0	0	F1,F2,F4
0	0	0	1	0	F1,F3,F4
1	0	1	1	0	F2,F3,F4
0	1	1	1	0	F1,F2,F3,F4

An electronic circuitry using an 8 bits microcontroller with a serial interface (RS232) and an Ethernet interface (10 Mbit/s) was designed for controlling the optical switches. The Ethernet interface allows the circuitry to be controlled remotely over the world wide web. The control table is implemented by software in the microcontroller, which then activates the optical switches by means of the corresponding device voltages. The circuitry board has also four LEDs that give the status of the selected channels. Fig. 6 shows a picture of the assembled OADM.

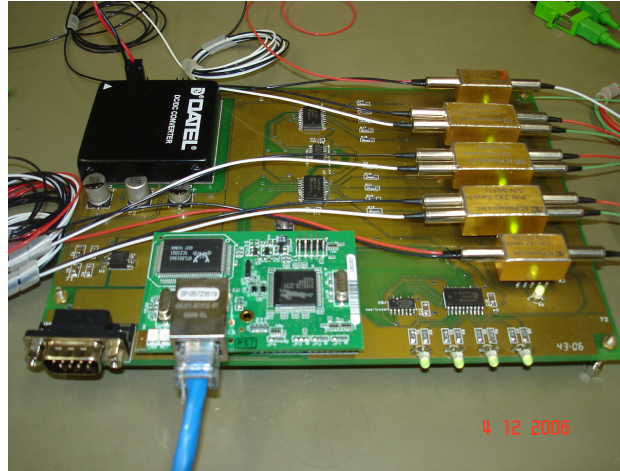


Fig. 6. Photo of the assembled circuitry with the microcontroller board on top of the main board.

For testing the OADM a C+L Band ASE Broadband source, with 1567.3 nm center wavelength and 10 dB bandwidth = 84.6 nm, is used at the OC 1 input port. When none channel is selected (all switches set to the “1” state) the insertion loss is minimum and measured as 5 dB at the output port of OC2. The upper solid line in Fig. 7 shows the source output as measured by the OSA, which is taken as the reference. The dashed line shows the situation where none channel is selected (measured at the OC2 output port). The four other curves show the reflected grating spectrum when each channel is selected individually. In this case the insertion loss increases depending on the selected wavelength as the return optical path will be different. The different spectra correspond to the individual reflection shape of the gratings used in the OADM. Furthermore, by dropping two or more channels simultaneously, the dropped channels will not remain power equalized. Since the drop port is located at the input OC1 circulator, the dropped channel corresponding to the grating nearest to the OC2 will have the greater attenuation.

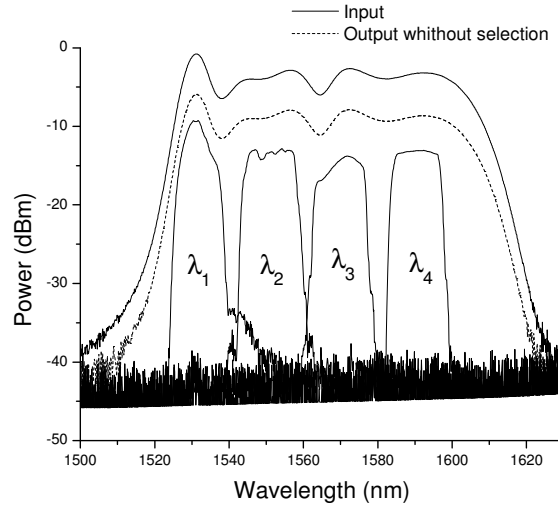


Fig. 7. Spectra of the input, output when none channel is selected (dashed line) and the dropped (λ_1 , λ_2 , λ_3 , and λ_4) channels when each channel is selected individually

The OADM response time is particularly limited by the response of the optical switches. The response time was checked by applying the corresponding voltages individually and jointly on the switches. The test was performed by placing a photodetector at the OC 1 drop port, whose signal was then acquired by a digital oscilloscope (Tektronix TDS 1002) with the help of an edge trigger. According to the manufacturer, the nominal response is < 4 ms for the 1x2 switch and < 10 ms for the 2x2 switch. However results have shown generally a much less response time. For example, Fig. 8 shows the response of the switch that actuates on the 1590 nm grating. In this particular case, the rise time is less than 300 μ s.

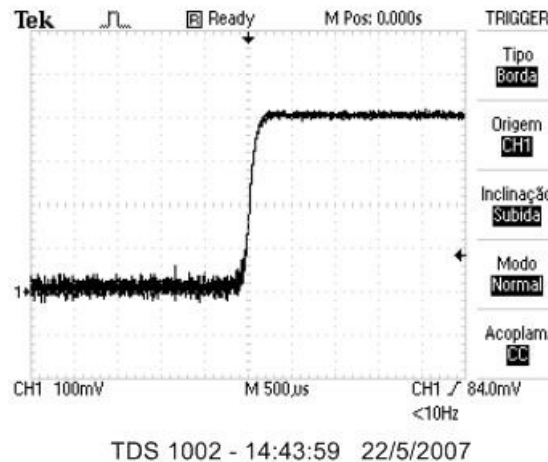


Fig. 8. Response time of the switch of the assembled circuitry with the microcontroller board on top of the main board.

V. CONCLUSION

Large bandwidth fiber gratings were successfully fabricated using a chirped phase mask and a step by step process in which several subgratings are inscribed and concatenated on the side of each other. However, a more accurate concatenation is not possible with the present fabrication setup, leading to small and narrow transmission bands on the saturated portion of the grating spectrum. The gratings present reflection spectra with a FWHM bandwidth that can be tailored from 7 up to 16nm, and with peak reflectivity in the range from -20 to -25dB. The magnitude of the reflected signal presents an almost flat top spectrum, an indication that the strength of the grating is very high. This is caused by the saturated hydrogen loading and by the over-exposure to the UV-beam. The gratings were employed as CWDM filters in a test bench and the BER test revealed a performance comparable to filters based on commercial thin film technology at the 2.5 Gbps rate. Although the filters were bench-tested, it is necessary to evaluate the BER performance of the OADM in an optical link, which could not be accomplished so far. An arrangement similar to the one shown in Fig. 3 can be used with the optical circulator and CWDM filter replaced by the OADM. Additionally, one requires optical amplifiers at the exit of the channel bank and at the entrance of the BER analyzer and spans of optical fiber with the OADM in-between. The fiber and the OADM insertion loss can be compensated for by the optical amplifiers so that the influence of channel cross-talk, generated by the use of several filters, can be evaluated. Considering the best value of measured insertion loss (-35 dB) for the filters, it is not expected that BER will be severely degraded due to cross-talk, if filters with such specifications are used in the OADM. As a comparison, 10^{-9} BER degradation at 2.5 Gbps due to cross-talk in FBG OADMs with 50 GHz channel separation is kept below 0.1 dB for the dropped channel in DWDM links [17], a condition that is much more critical than the channel separation found in CWDM networks.

A reconfigurable 4-Channel OADM was also assembled using the large bandwidth fiber Bragg gratings using commercial 1x2 and 2x2 optical switches. Due to the configuration of the OADM, in which gratings and switches are positioned in a row, the performance of the multiplexer reveals that the signal will not remain power equalized at the output when channels are dropped simultaneously, which is a result of the different paths followed by the signal through the device. The high insertion loss observed in the tests can also be reduced by an estimated 2.4 dB using splicing between the fiber patches in replacement of connectors used in the present configuration. Another possible arrangement could employ the CWDM filters in a parallel configuration, such as the one used in [18]. The advantage of such configuration lies on the fact that a better power balance among channels at the OADM output can lead to an improved link optical Signal-to-Noise ratio (OSNR). However, total insertion loss for a reconfigurable OADM would not be necessarily lower due to the use of several optical couplers and switches. Even the parallel 4-channel configuration reported in [18] points out to

an average insertion loss of 4 dB in the pass state (when none channels are selected), which is not lower than the serial configuration described in this work.

An attractive configuration for CWDM networks could use tunable CWDM FBG filters. However, as one needs to tune channels separated by 20 nm, only techniques that use compression loads applied to the grating are suited [19].

ACKNOWLEDGMENT

The authors thank Dr. J. B. Rosolem from Fundação CPqD, Brazil, for helping with the BER and isolation measurements. This work was supported by FUNTTEL/FINEP in Brazil by means of the GIGA project.

REFERENCES

- [1] ITU-T G694.2, "Spectral Grids for WDM Applications: CWDM Wavelength Grid", 2002.
- [2] Y. Li; L. Lee, D. Wang, L. Ji; J. Li; F. Wu, W.-S. Tsay, "Performance of an ultra-low loss, ultra compact, free-space packaging platform for CWDM applications", in *Digest of the LEOS Summer Topical Meetings*, pp. 28-30, 2004.
- [3] S. Bidnyk, A. Balakrishnan, M. Pearson, M. Gao and T. Hall, "Configurable coarse wavelength division demultiplexers based on planar reflective gratings", *Opt. Communications*, vol. 262, pp. 82-86, 2006.
- [4] C. R. Doerr, M. Capuzzo, L. Gomes, E. Chen, A Wong-Foy, C. Ho, J. Lam and K. McGreer, "Planar lightwave circuit eight-channel CWDM multiplexer with < 3.9 insertion loss", *J. Lightwave Technol.*, vol. 23, no. 1, pp. 62-65, 2005.
- [5] P.T. Neves Jr, P.V. Cosmo, F. Kuller, A.A.P. Pohl, H.J. Kalinowski, and J.L. Fabris, "4-Channel reconfigurable CWDM OADM based on FBG gratings", in *Proceedings of the 6th Conference on Telecommunications*, pp. 173-176, Peniche, Portugal, 2007.
- [6] R. Kashyap, P. F. Mckee, R. J. Campbell and D. L. Williams, "A novel method of writing photo-induced chirped Bragg gratings in optical fibers", *Electron. Lett.*, 30, pp. 996, 1994.
- [7] M. J. Cole, W. H. Loh, R. I. Laming, M. N. Zervas and S. Barcelos, "Moving fibre/phase-mask scanning beam technique for enhanced flexibility in producing fibre gratings with uniform phase-mask", *Electron. Lett.*, 31, pp. 1488-1489, 1995.
- [8] A. Asseh, H. Storoy, B.E. Sahlgren, S. Sandgren and R.A.H. Stubbe, "A writing technique for long fiber Bragg gratings with complex reflectivity profiles", *J. Lightwave Technol.*, vol. 15, no. 8, pp. 1419-1423, August 1997.
- [9] J. F. Brenann III, M. R. Matthews, W. V. Dowers, D. J. Treadwell, W. Wang, J. Porque, and X. Fan, "Dispersion correction with a robust fiber grating over the full C-band at 10 Gbps rates with a < 0.3 dB power penalties", *IEEE Photon. Techn. Lett.*, 15, pp. 1722-1724, 2003.
- [10] H. Rourke, B. Pough, S. Kanellopoulos, V. Baker, B. Napier, D. Greene, D. Goodchild, J. Fells, R. Eppworth, A. Collar and C. Rogers, "Fabrication of extreme long fibre gratings by phase-matched concatenation of multiple short sections", in *Proceedings of Bragg Gratings, Photosensitivity, and Poling in Glass Waveguides*, 23-25 September, Florida, pp. 32-34, 1999.
- [11] L. Paccou, P. Niay, L. Bigot, M. Douay, and I. Riant, "Nano-positioning of a Bragg grating inscription setup for the concatenation of multiple gratings using the diffractant experienced by the ultraviolet inscription beam", *Optics and Lasers in Engineering*, vol. 43, pp. 143-149, 2005.
- [12] Y. Wang, J. Grant, A. Sharma, G. Myers, "Modified Talbot interferometer for fabrication of fiber-optic grating filter over a wide range of Bragg wavelength and bandwidth using a single phase mask", *J. Lightwave Technol.*, vol. 19, pp. 1569-1573, 2001.
- [13] R. Kashyap, *Fiber Bragg Gratings*, Academic Press, London, 1999.
- [14] A Othonos and K Kalli; *Fiber Bragg Gratings*, Artech House, Norwood, 1999.
- [15] R.T. Zheng, N.Q. NGO, L.N. Binh, S.C. Tjin and J.L. Yang, "Chirped fiber Bragg gratings with arbitrary group delay responses using stepped-stretching fiber method", *Appl. Phys. B*, vol. 82, pp. 59-63, 2006.
- [16] S. Liaw, K. Ho and S. Chi, "Multichannel add/drop and cross-connect using fiber Bragg gratings and optical switches", *Electronics Letters*, vol. XXXIV, no. 16, pp. 1601-1603, 1998.
- [17] P. S. André, J. L. Pinto, I. Abe, H. J. Kalinowski, O. Frazão, F. M. Araujo, "Fibre Bragg grating for telecommunications applications: tunable thermally stress enhanced OADM", *Journal of Microwaves and Optoelectronics*, vol. 2, no. 3, pp. 32-45, 2001.
- [18] Q. Huang, F. Luo, J. Huo, Z. Wang, and M Xia, "Fully reconfigurable optical add-drop multiplexer based on parallel configuration using Mach-Zehnder module", *Optics Communications*, vol. 269, no. 1, pp. 113-118, 2007.

- [19] N. Mohammad, W. Szyszowsky, W. J. Zhang, E. I. Haddad, J. Zou, W. J. Jamroz, and R. Kruzelecky, "Analysis and development of a tunable fiber Bragg grating filter based on axial tension/compression," *J. Lightwave Technol.*, vol 22, no. 8, pp. 2001-2013, August 2004.